

Tip-enhanced single molecule fluorescence near-field microscopy in aqueous environment

Heinrich G. Frey,^{a)} Jan Paskarbeit, and Dario Anselmetti

Experimental Biophysics and Applied Nanoscience, Bielefeld University, Universitätsstraße 25, 33615 Bielefeld, Germany

(Received 4 May 2009; accepted 26 May 2009; published online 18 June 2009)

For nanobiophysical applications, scanning near-field optical microscopy must combine high optical resolution and single fluorescent molecule sensitivity with the ability to operate in aqueous solution. These requirements can be achieved using the electric field enhancement at the tip of illuminated silicon probes for atomic force microscopy (AFM), whereby single ATTO-740 dye molecules could be imaged at an optical resolution down to 20 nm under ambient conditions as well as in aqueous solution. Two illumination modes have been tested: (a) bottom illumination in a total internal reflection microscopy setup and (b) direct top illumination, both with dedicated phase-sensitive single photon counting technology in dynamic AFM mode of operation. © 2009 American Institute of Physics. [DOI: 10.1063/1.3155190]

Scanning near-field optical microscopy (SNOM) is an imaging technique operating at subwavelength dimensions.¹ Tip-enhanced SNOM (Ref. 2) is very promising, as it combines high optical resolution with high topographical resolution. For measurements in ambient environment, sub-10-nm resolution at good signal-to-noise ratio (SNR) up to 25.5 has been demonstrated.³ But for most nanobiological applications, the ability to work in aqueous environment is mandatory and has only been shown for sophisticated probes, e.g., a gold sphere attached to a glass tip.⁴ In this paper, we show that it is also possible to image single fluorescent molecules by tip-enhanced SNOM in aqueous environment with commercial Si cantilevers. Additionally, we compare different illumination modes and discuss their properties.

In tip-enhanced SNOM experiments,^{3,5–15} a bottom-illumination setup is generally used. Thereby, focused optical evanescent fields are generated by total internal reflection at a glass surface [Fig. 1(b)]. Although this bottom-illumination mode (BIM) yields remarkable advantage in light confinement and background reduction, it has the disadvantage of being restricted to thin samples as the probing tip must stay close to the glass surface. Only rarely and mostly in connection with tip-enhanced Raman spectroscopy,^{16,17} a top-illumination mode (TIM) [Fig. 1(a)] has been used. But it has the advantage that because it can also be applied to thicker samples such as cells or in experimental setups, where oil immersion objectives cannot be used. In this paper, we demonstrate that in TIM a similar SNR can be achieved as in BIM.

Our self-built SNOM setup combines BIM with TIM and allows operation in ambient and in aqueous environment [see Figs. 1(a) and 1(b)]. For bottom illumination, we use an oil immersion objective with a numerical aperture (NA) of 1.45 (Olympus, PlanApo TIRFM), where only a section of about 1/4 of the aperture is illuminated. For top illumination, we use an aspherical lens which has a NA of 0.42 in air (Thorlabs, 350350). The silicon cantilever probe (Nanosensors, ATEC-NC-20) is driven in tapping mode of opera-

tion with a constant tapping amplitude of about 50 nm. This amplitude combines repulsive contact with optical near-field excitation and pure far-field excitation in one oscillation cycle. The corresponding fluorescence signals are detected by a single avalanche photodiode (PerkinElmer, SPCM-AQR-13) and are electronically switched and fed into two independent digital counters corresponding to near-field and far-field, respectively [Fig. 1(c)]. Whereas one counter is enabled while the sample is in the cantilever's optical near-field, yielding the near-field signal with background contributions from the far-field, the other counter is enabled while the cantilever is at the top reversal point detecting the pure far-field background. A corrected near-field image is now calculated by subtracting the far-field background image from the near-field image. To reduce noise, we additionally low-pass filter the background image line by line before subtracting it. In order to reduce photobleaching of the dye molecules, the illumination laser (Roithner Lasertechnik

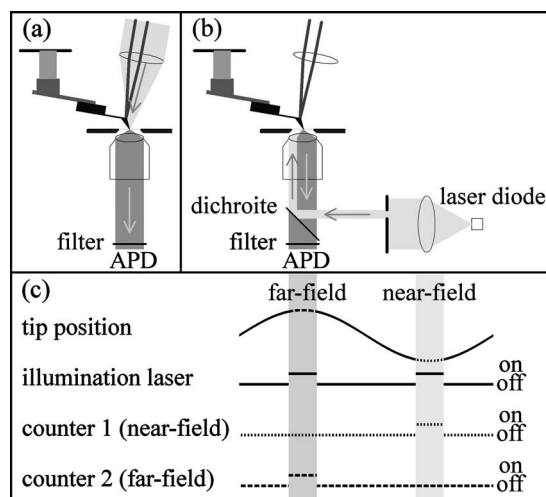


FIG. 1. SNOM setup with two illumination modes. (a) TIM. (b) BIM. To achieve high field enhancement, only a section of the lens aperture is illuminated. In both cases, the polarization must be parallel to the section plane and the fluorescence is collected in transmission via the object lens. (c) Optical information (single photon counting) is detected, tip position dependent.

^{a)}Electronic mail: hfrey@physik.uni-bielefeld.de.

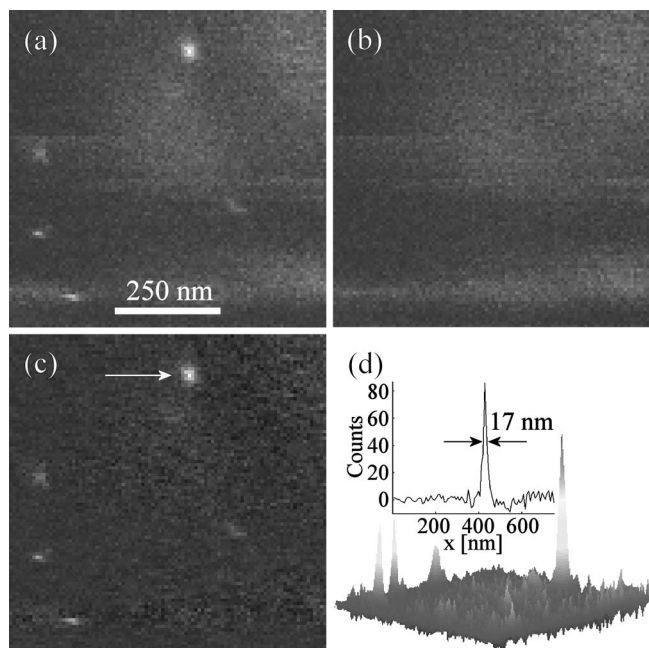


FIG. 2. SNOM image (BIM) of individual ATTO-740 molecules in water attached to a glass surface. (a) Fluorescence near-field image of single molecules with a diffuse background resulting from the far-field illumination. (b) Fluorescence far-field image. It shows only the background. (c) Background corrected near-field image. (d) 3d image of (c) and a cross-section through a single dye image with a FWHM of 17 nm.

GmbH, RLT6830MG, $\lambda=685$ nm) is oscillation-triggered turned on for the small phase windows of 40° while either one of the counters is enabled.

We have chosen ATTO 740 (ATTO-TEC) as fluorescent dye, as it exhibits a remarkable photostability and a small quantum efficiency of only 0.1. The small quantum efficiency is advantageous¹⁸ since it can increase when the radiative decay rate is enhanced by the tip. For measurements in aqueous solution, it is important that the single molecules are well bound to the glass surface. Otherwise, floating dye molecules will pass through the laser focus and give rise to fluorescent bursts. In principle, these fluorescent bursts can be well suppressed by subtracting the far-field background image, but we found that they introduce additional unwanted noise. Therefore, our samples were prepared in the following way: ATTO 740 NHS-ester is dissolved in waterless dimethylsulfoxide (DMSO) to a concentration of 100 ng/ml. A glass cover slip is cleaned by dipping it into 65% nitric acid and then successively rinsing it by water, acetone, ethanol, water, and ethanol, and blown dry with nitrogen gas. Then, the cover slip is dipped for 20 min into solution of toluene and 0.2% (3-aminopropyl)triethoxysilane, followed by successive rinsing in toluene, acetone, ethanol, water, and ethanol, and again blown dry with nitrogen gas. A droplet of 0.1 ml of dye solution is put onto the cover slip, incubated for 2 min and then washed off by DMSO. To get rid of unbound dye molecules, the sample is dipped into ultrasonic baths of DMSO for 5 min twice successively. Finally, the remaining DMSO is washed off by water and ethanol and the sample is blown dry with nitrogen gas.

In Fig. 2, fluorescence SNOM images of single ATTO-740 molecules are shown. These were measured in BIM in water. The individual images (a)–(c) illustrate the steps how near-field signals can be separated from the background. Full

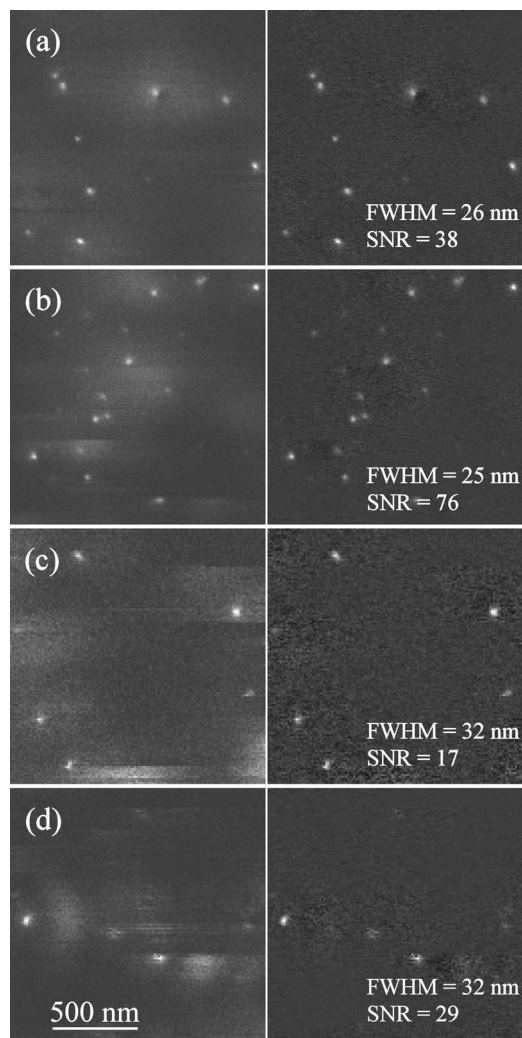


FIG. 3. SNOM image of individual ATTO-740 molecules. Left images always correspond to the measured near-field images whereas the images on the right correspond to the background corrected near-field image, respectively. All images were taken with the identical cantilever, but under different conditions: (a) Top illumination, in air. (b) Bottom illumination, in air. (c) Top illumination, in water. (d) Bottom illumination, in water.

width at half maximum (FWHM) of the imaged molecules could be determined to be less than 20 nm (here 17 nm). In order to compare both illumination modes and the change of environment, Fig. 3 shows images of single molecules detected with the identical cantilever in air as well as in water and for both illumination modes, respectively, where the measured near-field images are presented on the left side and the background corrected images on the right side. Interestingly, single molecule SNOM images, measured with tip-enhanced Si probes, show primarily single peaks. This is in contrast to metal tips, where single molecule images often show double-peaked patterns that depend on the orientation of the dye's dipole moment.^{19,20} This can be rationalized, since in the case of metal tips, fluorescence is quenched when the tip is directly over the dye molecule. So the patterns are dominated by the horizontal electrical field components which are located sidewise at the tip. In contrast, silicon tips generate fluorescence patterns that are dominated by the vertical electrical field component as the quenching effect is much weaker—there might even be enhanced emission.

The peak width and thus the resolution do not depend on the illumination mode. But the FWHM on average is slightly

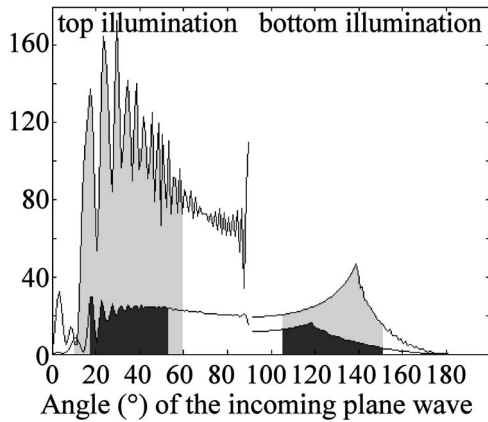


FIG. 4. Calculated enhancement of $|E|^2$ [multiple dipole method (Ref. 21)]. The electrical field was calculated 2 nm below a 20 μm long Si tip of rotational symmetry and a tip radius of 5 nm which is positioned 4 nm above a glass surface. The incoming plane wave is p -polarized, $\lambda=685$ nm. The upper line shows the enhancement in air, the lower line in water.

smaller in air (25 ± 6 nm) than in water (32 ± 7 nm). The single molecule SNOM images of Fig. 3 exhibit an SNR up to 76 in air and up to 29 in water. As the SNR depends strongly on the total signal, it is better to use the signal-to-background ratio (SBR) to compare the different imaging conditions since the images were taken at different illumination intensities. But since also the SBR was found to vary strongly from one single molecule image to another under the same conditions, we estimated the ratio of detected photons stemming from near-field interactions relatively to the total number of fluorescence photons. This can be calculated as $(I_{\text{down}} - I_{\text{up}})/(I_{\text{down}} + I_{\text{up}})$, where I_{down} and I_{up} are the integrals over the dark count corrected photon intensity images. The photon dark count was determined from fluorescence free areas within the SNOM images. The fractions are similar for all conditions: (a) (TIM, air) 0.030, (b) (BIM, air) 0.038, (c) (TIM, water) 0.036, and (d) (BIM, water) 0.027, respectively. These calculated fractions and peak widths now allow a direct comparison of the average SBR in air and in water: $\text{SBR}(\text{air})/\text{SBR}(\text{water})=1.7 \pm 0.5$. Interestingly, this value is slightly better than we would have expected from multiple dipole simulation calculations²¹ of the enhancement of $|E|^2$ under a silicon tip (Fig. 4). This may result from

simplifications of the probe geometry and from the fact that also the emission properties depend on the environment.

In summary, we could prove that tip-enhanced SNOM with silicon probes can be used to image single dye molecules in aqueous environment at high SNR and optical resolution down to 20 nm. For the identical tip, resolution and SBR are slightly decreased when comparing results in water to those in air. In addition, we show that the TIM gives results of similar quality as for bottom illumination. In both cases, it is expected that the background suppression can be further improved—in the case of bottom illumination by using radial polarized laser beam and in the case of top illumination by increasing the NA of the focusing lens.

- ¹D. Richards, *Philos. Trans. R. Soc. London, Ser. A* **361**, 2843 (2003).
- ²A. Hartschuh, *Angew. Chem., Int. Ed.* **47**, 8178 (2008).
- ³Z. Ma, J. M. Gertrion, L. A. Wade, and S. R. Quake, *Phys. Rev. Lett.* **97**, 260801 (2006).
- ⁴C. Höppener and L. Novotny, *Nanotechnology* **19**, 384012 (2008).
- ⁵E. J. Sánchez, L. Novotny, and X. S. Xie, *Phys. Rev. Lett.* **82**, 4014 (1999).
- ⁶T. J. Yang, G. A. Lessard, and S. R. Quake, *Appl. Phys. Lett.* **76**, 378 (2000).
- ⁷H. F. Hamann, M. Kuno, A. Gallagher, and D. J. Nesbitt, *J. Chem. Phys.* **114**, 8596 (2001).
- ⁸N. Hayazawa, Y. Inouye, and S. Kawata, *J. Microsc.* **194**, 472 (1999).
- ⁹J. Azoulay, A. Débarre, A. Richard, and P. Tchénio, *J. Microsc.* **194**, 486 (1999).
- ¹⁰A. Kramer, W. Trabesinger, B. Hecht, and U. P. Wild, *Appl. Phys. Lett.* **80**, 1652 (2002).
- ¹¹A. Hartschuh, E. J. Sánchez, X. S. Xie, and L. Novotny, *Phys. Rev. Lett.* **90**, 095503 (2003).
- ¹²T. Ichimura, N. Hayazawa, M. Hashimoto, Y. Inouye, and S. Kawata, *Phys. Rev. Lett.* **92**, 220801 (2004).
- ¹³V. V. Protasenko, A. Gallagher, and D. J. Nesbitt, *Opt. Commun.* **233**, 45 (2004).
- ¹⁴V. V. Protasenko and A. Gallagher, *Nano Lett.* **4**, 1329 (2004).
- ¹⁵J. M. Gerton, L. A. Wade, G. A. Lessard, Z. Ma, and S. R. Quake, *Phys. Rev. Lett.* **93**, 180801 (2004).
- ¹⁶B. Pettinger, B. Ren, G. Picardi, R. Schuster, and G. Ertl, *Phys. Rev. Lett.* **92**, 096101 (2004).
- ¹⁷J. Steidtner and B. Pettinger, *Phys. Rev. Lett.* **100**, 236101 (2008).
- ¹⁸J. R. Lakowicz, Y. Shen, S. D'Auria, J. Malicka, J. Fang, Z. Gryczynski, and I. Gryczynski, *Anal. Biochem.* **301**, 261 (2002).
- ¹⁹H. G. Frey, S. Witt, K. Felderer, and R. Guckenberger, *Phys. Rev. Lett.* **93**, 200801 (2004).
- ²⁰H. G. Frey, C. Bolwien, A. Brandenburg, R. Ros, and D. Anselmetti, *Nanotechnology* **17**, 3105 (2006).
- ²¹L. Novotny, *Appl. Phys. Lett.* **69**, 3806 (1996).